Original Article

DOI: 10.4274/haseki.galenos.2026.52714
Med Bull Haseki 2026;64(4):324-332

Ocular Surface and Meibomian Gland Phenotypes in Early-onset versus Late-onset Rheumatoid Arthritis: A Retrospective, Cross-sectional Comparative Imaging Study

Iffet Merve Ucar Baytaroglu[1], Ata Baytaroglu[2]

[1]*Usak Training and Research Hospital, Clinic of Rheumatology, Usak, Türkiye*
[2]*Usak Training and Research Hospital, Clinic of Ophthalmology, Usak, Türkiye*

Abstract

Aim: Ocular surface involvement in rheumatoid arthritis (RA) is well documented; however, the role of age at onset has not been characterized using modern topographic imaging. We compared ocular surface and meibomian gland phenotypes among early-onset RA (EORA), late-onset RA (LORA), and healthy controls, and related these phenotypes to systemic inflammatory and serologic features.

Methods: This single-center, retrospective, cross-sectional study (October 2022-September 2025) enrolled 126 age-matched participants: EORA, LORA, and healthy controls (n=42 per group). Rheumatoid arthritis was diagnosed according to the 2010 American College of Rheumatology/European League Against Rheumatism criteria. All participants completed the Ocular Surface Disease Index questionnaire and underwent slit-lamp biomicroscopy, Schirmer I testing, and Sirius+ topography to assess non-invasive break-up time, tear film thickness, and infrared meibography. 28-joint Disease Activity Score, rheumatoid factor, anti-cyclic citrullinated peptide, and antinuclear antibody status were recorded. Kruskal-Wallis test with Dunn-Bonferroni post-hoc comparisons, and chi-square or Fisher's exact tests were applied ($p<0.05$).

Results: Meibomian gland atrophy showed a trend toward higher values in EORA than in controls [33.0% (interquartile range 25.0-43.0) vs. 18.0% (10.0-35.8); $p=0.076$ after Bonferroni correction]. Ocular Surface Disease Index differed markedly across groups (EORA 41.0; LORA 15.0; controls 7.0; $p<0.001$). Tear film thickness was greatest in LORA (240.0 µm) and lowest in EORA (180.0 µm; $p=0.049$). Seropositivity was highest in EORA (80.0%) compared with LORA (63.2%) and controls (23.1%; $p<0.001$). Smoking was more frequent in LORA (28.6%) than in EORA (4.8%; $p=0.011$). 28-joint Disease Activity Score, erythrocyte sedimentation rate, and C-reactive protein did not differ between RA groups.

Conclusion: Despite comparable systemic disease activity, EORA and LORA appear to represent two distinct ocular surface phenotypes. Early-onset RA was associated with symptomatic presentation, seropositivity, and a trend toward greater meibomian gland atrophy, whereas LORA showed tear film instability, higher smoking exposure, and lower symptom reporting. Objective meibography, rather than symptom scoring alone, may help avoid underdiagnosis in older-onset RA.

Keywords: Arthritis, rheumatoid, age of onset, dry eye syndromes, meibomian glands, meibomian gland dysfunction, tear film

Corresponding Author: Ata Baytaroglu, MD, Usak Training and Research Hospital, Clinic of Ophthalmology, Usak, Türkiye
E-mail: baytaroglua@gmail.com **ORCID:** orcid.org/0000-0003-1993-0403
Received: 30.11.2025 **Accepted:** 27.07.2026 **Publication Date:** 24.09.2026

Cite this article as: Ucar Baytaroglu IM, Baytaroglu A. Ocular surface and meibomian gland phenotypes in early-onset versus late-onset rheumatoid arthritis: a retrospective, cross-sectional comparative imaging study. Med Bull Haseki. 2026;64(4):324-332

Introduction

Rheumatoid arthritis (RA) is a chronic, systemic inflammatory disease that primarily affects the synovial joints but also injures highly vascularized extra-articular tissues, including the ocular surface (1). Recent epidemiologic data place the global RA prevalence between 0.5% and 1.0% and confirm a steady rise in older-onset cases as populations age (2). Two clinical entities are now recognized on the basis of age at disease onset: [early-onset RA (EORA), onset <60 years] and [late-onset RA (LORA), onset ≥60 years], and recent reviews position LORA as a pathogenically distinct subset driven by immunosenescence, inflammaging, and clonal hematopoiesis rather than by classical autoimmunity (3,4). A 2026 systematic review and meta-analysis of more than 5,000 patients reported persistently higher post-treatment 28-joint Disease Activity Score (DAS28) scores and lower biologic-induced remission rates in LORA, supporting the view that age at onset modifies both immune phenotype and therapeutic response (5).

Ocular surface and meibomian gland involvement in RA has been described, but the relative contribution of EORA versus LORA remains poorly characterized in modern imaging studies. Comparative work to date has focused on joint and systemic features, with sonographic and clinical studies suggesting more active synovitis and a higher comorbidity burden in LORA, while autoantibody load and erosive disease tend to predominate in EORA (6,7). The eye-related literature has largely treated RA as a single disease, with ocular involvement reported in 28-55% of patients and ranging from mild keratoconjunctivitis sicca to vision-threatening peripheral ulcerative keratitis (8,9). Quantitative meibography, which directly visualizes acinar atrophy, has rarely been applied to the EORA versus LORA comparison, and the interaction with smoking exposure, an established environmental driver of citrullination and ocular surface damage, has not been systematically addressed (10).

We hypothesized that despite comparable systemic disease activity, EORA and LORA patients would display measurably different ocular surface phenotypes, with EORA showing more aggressive meibomian gland atrophy and higher subjective symptom burden and LORA showing tear film instability that is partially masked by reflex tearing related to environmental smoking. The aim of this retrospective, age-matched, single-center study was to compare ocular surface and meibomian gland imaging parameters between EORA, LORA, and healthy controls and to relate the findings to the autoantibody profile, smoking status, and DAS28-based disease activity. We aimed to provide phenotype-specific guidance for ophthalmologists managing RA patients, particularly the under-recognized LORA subgroup.

Materials and Methods

Compliance with Ethical Standards

This study was approved by the Usak University Non-Interventional Studies Ethics Committee (approval number: 907-907-12, date: 23.10.2025) and conducted in accordance with the principles of the Declaration of Helsinki. All patient identifiers were removed before analysis. The authors declare no conflict of interest. The study received no external funding.

Study Design

This was a single-center, retrospective, cross-sectional, comparative imaging study conducted in the Departments of Ophthalmology and Rheumatology at Usak University Training and Research Hospital between October 2022 and September 2025. Records of consecutive RA patients and age-matched non-RA controls were screened and examined for refractive evaluation. The detailed participant flow is shown in Figure 1.

Participants and Eligibility Criteria

Three groups were enrolled: EORA (disease onset before 60 years of age, n=42), LORA (disease onset at or after 60 years of age, n=42), and age-matched healthy controls (n=42). The diagnosis of RA was based on the 2010 American College of Rheumatology/European League Against Rheumatism classification criteria, and patients had at least one year of follow-up. Inclusion required age ≥18 years and the ability to complete the Ocular Surface Disease Index (OSDI) questionnaire and Sirius+ imaging. Exclusion criteria were spherical equivalent exceeding ±3.00 D, prior ocular or eyelid surgery, long-term contact-lens wear, active ocular infection or inflammation other than RA-related changes, allergic or vernal/atopic keratoconjunctivitis, use of topical ocular medications other than non-preserved artificial tears within the preceding 3 months, and any corneal pathology that would interfere with topographic imaging. Only the right eye of each participant was analyzed to avoid inter-eye correlation.

Ophthalmic Assessment

All participants underwent a standardized ophthalmic examination by a single experienced clinician (A.B.), which included best-corrected visual acuity, autorefraction, slit-lamp biomicroscopy of the lids, conjunctiva, cornea, and tear film, intraocular pressure measurement, fluorescein staining with non-preserved dye, and the OSDI questionnaire. Schirmer I testing was performed without anesthesia, and values of <5 mm/5 min were recorded as positive for aqueous tear deficiency. Non-invasive break-up time and tear film thickness were measured using the Sirius+ topography system (CSO, Florence, Italy) with Phoenix software (version 4.1.3.1).

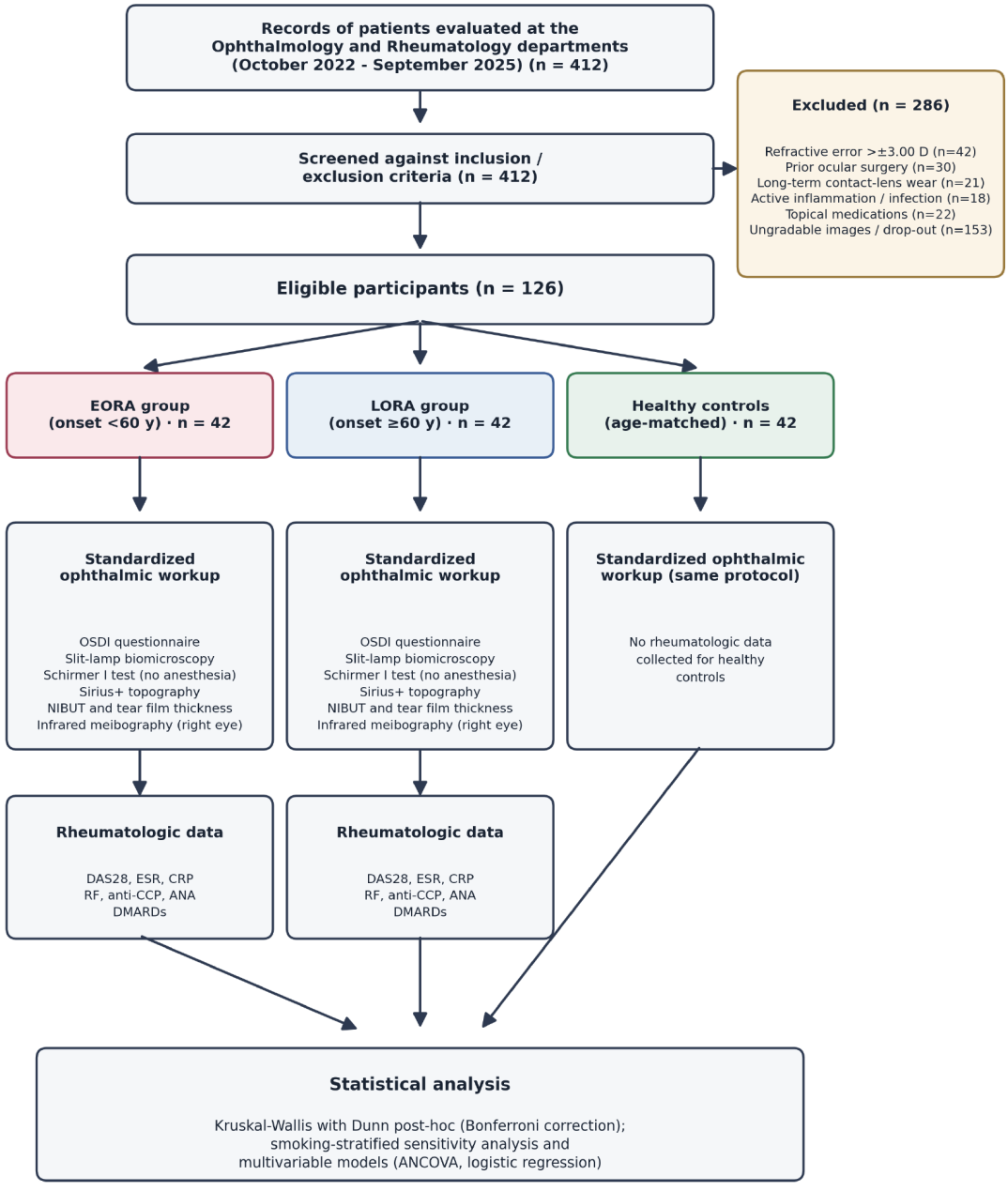

Figure 1. Study flow diagram. Flow of patients screened, excluded, enrolled, and analyzed in the EORA, LORA, and control groups. Standardized ophthalmic and rheumatologic workups were applied across the rheumatoid arthritis groups; healthy controls underwent the same ophthalmic protocol without rheumatologic data collection

EORA: Early-onset rheumatoid arthritis, LORA: Late-onset rheumatoid arthritis, OSDI: Ocular Surface Disease Index, NIBUT: Non-invasive break-up time, DAS28: 28-joint Disease Activity Score, ESR: Erythrocyte sedimentation rate, CRP: C-reactive protein, RF: Rheumatoid factor, anti-CCP: Anti-cyclic citrullinated peptide, ANA: Antinuclear antibody, DMARD: Disease-modifying anti-rheumatic drug

Meibography and Gland-atrophy Quantification

Infrared meibography was acquired using the meibography module embedded in the Sirius+ platform; the percentage of meibomian gland atrophy was automatically generated by the device's analysis software (Phoenix v.4.1.3.1) within the user-specified boundaries. The automatic atrophy estimation provided by the Sirius+ device shows good intra-device repeatability and segmentation performance comparable to recently validated convolutional-neural-network-based

meibography algorithms reported by Wang et al. (11) and Yesilirmak et al. (12), with semantic-segmentation Jaccard indices in the same range as those of expert graders (13). Each acquisition was screened for image quality (proper lid eversion, focus, and absence of motion blur) before automatic analysis, and unusable images were discarded and retaken.

Rheumatologic Assessment

For RA patients, disease duration, age at diagnosis, current and prior exposure to disease-modifying anti-rheumatic drugs (DMARDs), smoking status, and comorbidities were recorded. Laboratory parameters included rheumatoid factor (RF), anti-cyclic citrullinated peptide (anti-CCP), antinuclear antibody (ANA), erythrocyte sedimentation rate (ESR), and C-reactive protein (CRP) (Tables 1 and 2). Disease activity was assessed using the DAS28. Rheumatoid factor was measured by nephelometric assay and regarded as positive at the laboratory reference cut-off (>14 IU/mL); anti-CCP antibodies were measured by enzyme immunoassay and regarded as positive above the manufacturer's threshold (>17 U/mL). The same assays and cut-offs were applied to all participants, including controls, so that seropositivity in the control group reflects RF positivity at the standard diagnostic cut-off rather than low-titre or borderline reactivity. In the control group, serologic results were available only for participants for whom testing had been requested during routine evaluation, and this subset defined the denominator for control serology.

Statistical Analysis

An a priori power calculation for a one-way analysis of variance with three groups was conducted using G*Power v.3.1.9.2. An effect size of f=0.30, an alpha=0.05, and a power=0.80 indicated a minimum of 37 subjects per group; 42 subjects per group were enrolled to allow for exclusions. Distributional assumptions were assessed with Shapiro-Wilk testing; all primary continuous outcomes deviated from normality and were therefore analyzed with the Kruskal-Wallis test followed by Dunn post-hoc pairwise comparisons with Bonferroni correction. Categorical variables were compared using the chi-square or Fisher's exact test, as appropriate. Pre-specified sensitivity analyses were performed: a smoking-stratified Kruskal-Wallis comparison of tear film thickness, meibomian gland atrophy, and OSDI between EORA and LORA; and multivariable analysis of covariance and logistic regression adjusting for smoking and seropositivity (Tables 3 and 4). The analysis of covariance modeled each continuous ocular surface outcome (meibomian gland atrophy, tear film thickness, and OSDI), with group as the factor and smoking and seropositivity as covariates; logistic regression modeled seropositivity with group and smoking as predictors. Effect estimates [beta coefficients or odds ratios (ORs)] with 95% confidence intervals (CIs) are reported in Table 5. These multivariable models were secondary and were not corrected for multiple comparisons; thus, they complement rather than replace the Bonferroni-corrected primary analyses. Because of the moderate sample size and the marked imbalance in smoking prevalence between groups (4.8% in EORA vs. 28.6% in LORA), the multivariable models were considered supportive rather than demonstrating causality; results are reported with effect estimates and 95% CIs where appropriate. $p<0.05$ was considered statistically significant. Analyses were performed using GraphPad Prism v10.6.1 for macOS (GraphPad Software, Boston, MA, USA).

Results

A total of 126 participants were included (EORA n=42, LORA n=42, controls n=42). The median age was similar across groups [62.0 (60.5-63.5) years vs. 66.0 (61.0-71.0) years vs. 64.0 (62.0-66.0) years; p=0.06]. Demographic, serologic, and ocular surface variables are summarized in Tables 1-3 and Figure 2.

Table 1. Demographic, systemic, and ocular surface characteristics of early-onset (EORA), late-onset (LORA), and control groups

Variable	EORA (n=42)	LORA (n=42)	Controls (n=42)	p-value
Age (years)	62.0 (60.5-63.5)	66.0 (61.0-71.0)	64.0 (62.0-66.0)	0.060
ESR (mm/h)	21.0 (14.5-25.0)	21.0 (14.0-31.5)	n.a.	0.86†
CRP (mg/L)	6.2 (3.8-20.4)	6.5 (2.2-19.8)	n.a.	0.70†
DAS28	3.8 (2.7-4.6)	3.2 (2.7-4.1)	n.a.	0.59†
Meibomian gland atrophy (%)	33.0 (25.0-43.0)	26.0 (22.0-39.5)	18.0 (10.0-35.8)	0.035*
Tear film thickness (μm)	180.0 (115.0-230.0)	240.0 (200.0-315.0)	200.0 (180.0-245.0)	0.049*
NIBUT (s)	9.0 (6.0-12.0)	10.0 (6.0-12.0)	11.0 (7.3-14.0)	0.353
OSDI score	41.0 (18.5-45.5)	15.0 (11.0-24.5)	7.0 (3.3-12.0)	<0.001*

Values are median (interquartile range). Three-group comparisons used the Kruskal-Wallis test; †Indicates a two-group Mann-Whitney U test (EORA vs. LORA only) for biomarkers limited to the rheumatoid arthritis groups. *p<0.05
EORA: Early-onset rheumatoid arthritis, LORA: Late-onset rheumatoid arthritis, ESR: Erythrocyte sedimentation rate, CRP: C-reactive protein, DAS28: 28-joint Disease Activity Score, NIBUT: Non-invasive break-up time, OSDI: Ocular Surface Disease Index

Table 2. Distribution of categorical variables across groups				
Variable	**EORA (%)**	**LORA (%)**	**Controls (%)**	**p-value**
Male sex	23.8	26.2	38.1	0.872
Smoking	4.8	28.6	21.4	0.011*
Any comorbid disease	26.2	28.6	31.0	0.321
Diabetes mellitus	7.1	11.9	7.1	0.441
Hypertension	16.7	19.0	19.0	0.553
Coronary artery disease	4.8	7.1	23.8	0.107
Seropositivity (RF and/or anti-CCP)	80.0	63.2	23.1	<0.001*
RF positivity	73.3	63.2	23.1	<0.001*
Anti-CCP positivity	60.0	52.6	0.0	<0.001*
ANA positivity	40.0	31.6	15.4	0.193
Extra-articular involvement	7.1	0.0	0.0	0.076
Prednisolone use	21.4	16.7	0.0	0.300
Methotrexate use	14.3	23.8	0.0	0.510
Leflunomide use	19.0	14.3	0.0	0.296
Biologic DMARD use	4.8	2.4	0.0	0.571
Hydroxychloroquine use	4.8	9.5	0.0	0.672
Sulfasalazine use	4.8	0.0	0.0	0.187
Limbal hyperemia (score ≥1)	16.7	19.0	26.2	0.140
Positive Schirmer test (<5 mm/5 min)	9.5	7.1	0.0	0.030*

Categorical variables compared with the chi-square test or Fisher exact test as appropriate. *p<0.05
Serologic percentages were calculated among participants with available serology; in the control group, this denominator comprised only those tested during routine evaluation, and control seropositivity denotes rheumatoid factor positivity at the standard laboratory cut-off (>14 IU/mL), not low-titre reactivity
EORA: Early-onset rheumatoid arthritis, LORA: Late-onset rheumatoid arthritis, RF: Rheumatoid factor, anti-CCP: Anti-cyclic citrullinated peptide, ANA: Antinuclear antibody, DMARD: Disease-modifying anti-rheumatic drug

Table 3. Dunn post-hoc pairwise comparisons (Bonferroni correction) for variables with significant Kruskal-Wallis results				
Variable	**Comparison**	**Z**	**p-value**	**Bonferroni-adjusted p**
Meibomian gland atrophy (%)	EORA vs. LORA	0.56	0.578	1.000
	EORA vs. controls	2.24	0.025	0.076
	LORA vs. controls	1.99	0.047	0.140
Tear film thickness (μm)	EORA vs. LORA	2.24	0.025	0.075
	EORA vs. controls	1.55	0.121	0.363
	LORA vs. controls	1.40	0.163	0.490
OSDI score	EORA vs. LORA	2.37	0.018	0.055
	EORA vs. controls	>3.6	<0.001	<0.001*
	LORA vs. controls	3.40	<0.001	0.002*

Only variables with a significant Kruskal-Wallis p<0.05 entered the post-hoc analysis. *p<0.05 after Bonferroni correction
EORA: Early-onset rheumatoid arthritis, LORA: Late-onset rheumatoid arthritis, OSDI: Ocular Surface Disease Index

Table 4. Smoking-stratified sensitivity analysis of ocular surface outcomes between EORA and LORA non-smokers			
Variable	**EORA non-smokers (n=40)**	**LORA non-smokers (n=30)**	**p-value**
Meibomian gland atrophy (%)	33.5 (26.0-44.0)	25.0 (21.0-38.0)	0.046*
Tear film thickness (μm)	182.0 (118.0-232.0)	232.0 (198.0-306.0)	0.062
NIBUT (s)	9.0 (6.0-12.0)	10.5 (7.0-13.0)	0.412
OSDI score	41.5 (19.0-46.0)	16.0 (11.5-25.0)	<0.001*

Pre-specified sensitivity analysis restricted to never- or ex-smokers. Two-group comparison performed with the Mann-Whitney U test. *p<0.05
EORA: Early-onset rheumatoid arthritis, LORA: Late-onset rheumatoid arthritis, NIBUT: Non-invasive break-up time, OSDI: Ocular Surface Disease Index

Table 5. Multivariable models of ocular surface outcomes and seropositivity, adjusted for smoking and seropositivity				
Model	**Outcome/predictor**	**Estimate**	**Adjusted estimate (95% CI)**	**p-value**
ANCOVA	OSDI score (EORA vs. LORA)	β	27.7 (22.4 to 33.0)	<0.001
ANCOVA	Tear film thickness, μm (EORA vs. LORA)	β	-57.9 (-78.5 to -37.2)	<0.001
ANCOVA	Meibomian gland atrophy, % (EORA vs. LORA)	β	4.3 (0.1 to 8.5)	0.045
Logistic regression	Seropositivity: EORA vs. others	OR	5.7 (2.3 to 14.1)	<0.001
Logistic regression	Seropositivity: smoking	OR	1.3 (0.5 to 3.4)	0.58

Analysis of covariance (ANCOVA) estimates are beta coefficients (β) for the EORA versus LORA contrast (reference: LORA), adjusted for smoking and seropositivity; positive values indicate higher outcomes in EORA and the tear film thickness coefficient is negative because values were lower in EORA. Logistic regression estimates are odds ratios for seropositivity (rheumatoid factor and/or anti-CCP), adjusted for smoking. These secondary models were not corrected for multiple comparisons and complement the Bonferroni-corrected analyses in Table 3. CI: Confidence interval, OSDI: Ocular Surface Disease Index, EORA: Early-onset rheumatoid arthritis, LORA: Late-onset rheumatoid arthritis

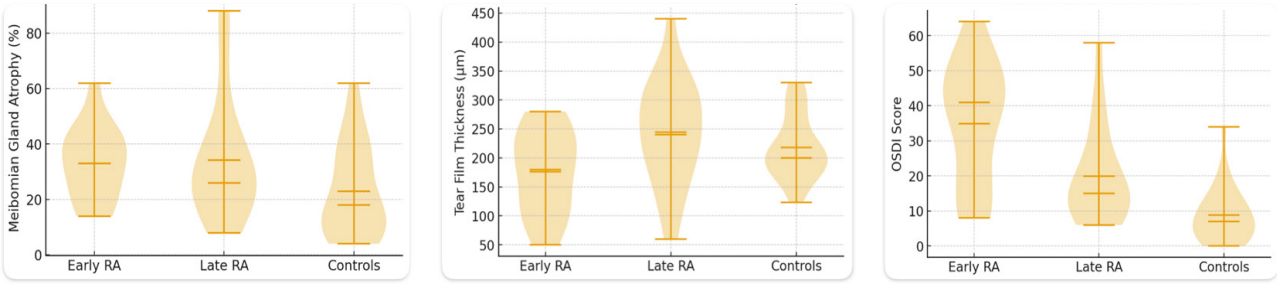

Figure 2. Violin plots of ocular surface parameters across the three groups. Distribution of meibomian gland atrophy (%), tear film thickness (μm), non-invasive break-up time (s), and Ocular Surface Disease Index score across EORA, LORA, and healthy controls. Boxes within violins represent medians and IQRs; whiskers show 1.5 × IQR. Three-group comparisons were performed with the Kruskal-Wallis test

EORA: Early-onset rheumatoid arthritis, LORA: Late-onset rheumatoid arthritis, IQR: Interquartile range, CI: Confidence interval, RA: Rheumatoid arthritis

Systemic disease activity did not differ between EORA and LORA [DAS28: 3.8 (2.7-4.6) vs. 3.2 (2.7-4.1), p=0.59; ESR, p=0.86; CRP, p=0.70]. Seropositivity (RF and/or anti-CCP) differed across groups (Figure 3): it was highest in EORA (80.0%), intermediate in LORA (63.2%), and lowest in controls (23.1%; p<0.001). Rheumatoid factor and anti-CCP each demonstrated the same gradient (both p<0.001). Antinuclear antibody positivity was highest in EORA (40.0%) but did not reach statistical significance (p=0.193).

Meibomian gland atrophy tended to be higher in the EORA group [33.0% (25.0-43.0)] than in controls [18.0% (10.0-35.8)]; overall Kruskal-Wallis p=0.035. The pairwise comparison did not remain significant after Bonferroni correction (EORA vs. control p=0.076). Tear film thickness differed across groups (p=0.049), with the highest median value in LORA [240.0 μm (200.0-315.0)] and the lowest in EORA [180.0 μm (115.0-230.0)]; no pairwise comparisons remained significant after Bonferroni correction (Table 3). Non-invasive break-up time did not differ between groups (p=0.353).

Ocular Surface Disease Index showed the largest between-group separation (p<0.001). EORA patients reported the highest symptom burden [median 41.0 (18.5-45.5)], LORA patients reported intermediate scores [median 15.0 (11.0-24.5)], and controls reported minimal symptoms [median 7.0 (3.3-12.0)]. Both RA groups had significantly higher OSDI scores than controls (adjusted p<0.001 for both). The EORA versus LORA comparison was borderline significant (adjusted p=0.055).

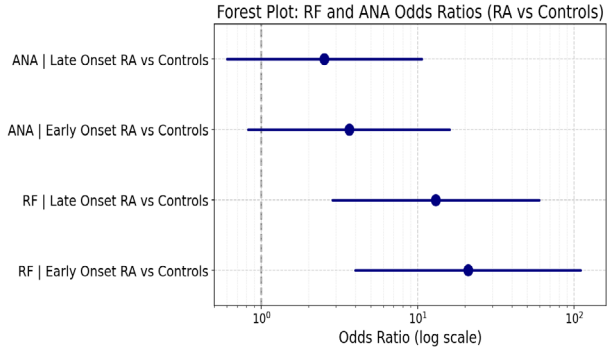

Figure 3. Forest plot of odds ratios for serologic positivity [rheumatoid factor (RF) and antinuclear antibody (ANA)] across rheumatoid arthritis subtypes versus healthy controls Odds ratios for RF and ANA positivity in EORA and LORA versus healthy controls, plotted on a logarithmic scale with 95% confidence intervals. RF positivity discriminates both RA subtypes from controls. ANA positivity shows a non-significant trend toward higher rates in RA

EORA: Early-onset rheumatoid arthritis, LORA: Late-onset rheumatoid arthritis, RA: Rheumatoid arthritis

Smoking prevalence differed across groups (4.8% in EORA, 28.6% in LORA, and 21.4% in controls; p=0.011). A positive Schirmer test was observed only in the RA groups (9.5% in EORA, 7.1% in LORA, and 0% in controls; p=0.030). In the pre-specified, smoking-stratified analysis restricted to non-smokers, EORA still exhibited higher meibomian gland atrophy and OSDI scores than LORA (Table 4), suggesting that the EORA phenotype was not explained by lower smoking exposure. In the multivariable models (Table 5), the estimates were directionally consistent with the unadjusted comparisons. After adjustment for smoking and seropositivity, OSDI remained higher in EORA than in LORA (adjusted β 27.7, 95% CI 22.4 to 33.0; p<0.001), and tear film thickness remained lower in EORA (adjusted β -57.9, 95% CI -78.5 to -37.2; p<0.001). The difference in meibomian gland atrophy was modest, with a CI that approached the null (adjusted β 4.3, 95% CI 0.1 to 8.5; p=0.045), consistent with a trend rather than a reliable independent effect. In the logistic model, seropositivity was associated with EORA (adjusted OR 5.7, 95% CI 2.3 to 14.1; p<0.001) but not with smoking (OR 1.3, 95% CI 0.5 to 3.4; p=0.58). Other comorbidities, DMARD exposure, and ANA status did not differ between EORA and LORA (Figure 3).

Discussion

An age-matched comparison of ocular surface and meibomian gland phenotypes between EORA and LORA cohorts using objective topographic imaging has not hitherto been reported. The pattern that emerged from our data was unforeseen in two respects. Early-onset RA showed a trend toward greater meibomian gland atrophy and significantly higher OSDI scores than both LORA and controls, although DAS28, ESR, and CRP were comparable across RA subgroups; this difference in atrophy did not remain significant after correction for multiple comparisons and was therefore interpreted as a trend. LORA, despite a sixfold higher smoking prevalence, had the thickest tear film and the lowest symptom burden among RA subgroups. Seropositivity for RF or anti-CCP, while elevated in both groups, tracked the EORA gland-atrophy phenotype more closely than the LORA phenotype.

Our observation that systemic disease activity scores fail to predict ocular surface severity aligns with the meta-analysis by Yang et al. (5), which found that LORA achieved remission less often than younger-onset RA on biologic and targeted synthetic DMARDs at comparable baseline DAS28. It also fits the framework of Ma et al. (3), who place the EORA/LORA distinction at the level of immune mechanism rather than at the level of joint count or acute-phase reactants. From this point of view, the ocular surface may offer a second readout of disease biology: in EORA, reflecting a phenotype associated with long-standing, seropositive, B-cell-related autoimmunity; in LORA, reflecting an older immune background in which environmental exposures may play a comparatively larger role. These interpretations describe associations rather than demonstrated mechanisms, because the retrospective design cannot establish causality.

The high seropositivity rates in our EORA group (RF 73.3%, anti-CCP 60.0%) are consistent with, but do not establish, a B-cell-related contribution to meibomian gland injury. Anti-citrullinated protein antibodies are increasingly recognized as drivers of tissue damage beyond the synovium, and citrullinated targets have been identified in the lacrimal gland and conjunctival epithelium. The preferential involvement of meibomian glands, which are sebaceous and androgen-regulated, may reflect several mechanisms acting together: direct autoantibody binding (14,15), long-term cytokine exposure [tumor necrosis factor alpha, interleukin (IL)-6, IL-17], and loss of androgen-mediated trophic support. All three are well documented in RA (16,17). These pathways were not directly assessed in the present study. Long-standing seropositive RA has been associated with extra-articular manifestations and exocrine gland involvement (18), and Targońska-Stępniak et al.'s (19) comparison of LORA and EORA reported a similar immune-aggression gradient at the systemic level, although ocular outcomes were not measured.

The LORA presentation, in which mild symptoms persist despite the absence of dry eye findings, warrants closer examination. Cigarette smoke is a well-characterized ocular surface toxin that destabilizes the lipid layer, depletes goblet cells, and reduces meibomian gland density (20). It is conspicuous that the magnitude of these effects in chronic smokers does not appear to depend on smoking duration or nicotine dependence in a dose-dependent manner (20). If smoking exerted a uniform pressure to increase glandular atrophy in our LORA group, the higher atrophy observed in EORA would be consistent with an autoimmune-related signal; however, this requires validation in a prospective study. Smoking-related compensatory reflex tearing in LORA may also explain the greater tear film thickness despite poorer underlying tear stability, an interpretation supported by recent immunological data linking smoking to preferential induction of mucosal IgA anti-citrullinated protein antibodies (21). Tear film hyperosmolarity has previously been reported as a feature of RA-related dry eye, with disease activity, treatment, and age contributing independently to ocular surface signs (22,23). In our pre-specified smoking-stratified sub-analysis, the difference in OSDI between EORA and LORA persisted among non-smokers, with a similar but weaker trend for meibomian gland atrophy.

The sign-symptom dissociation we observed has direct clinical implications. Early-onset RA patients reported severe symptoms (median OSDI score of 41), whereas LORA patients reported only mild symptoms (OSDI score of 15) despite the presence of moderate gland atrophy. Two mechanisms could plausibly explain this. Early-onset RA patients may develop corneal neuropathic pain and central sensitization against a background of long-standing systemic inflammation, which would align with the increased corneal Langerhans-cell density and reduced corneal nerve fiber length reported by Bitirgen et al. (24) in RA. Conversely, LORA patients may have blunted corneal nerve sensitivity due to immunosenescence, resulting in underreporting of objective gland loss on questionnaires. Symptom scoring alone may, therefore, underestimate ocular surface disease in LORA, and direct meibography is a more reliable screening tool than symptom scoring. Deep-learning meibography pipelines now achieve expert-level segmentation accuracy (11-13) and should reduce operator dependence in routine use.

Our results also align with the gerontological view of difficult-to-treat RA from Lehoczki et al. (4), in which cumulative organ vulnerability, polypharmacy, and frailty determine outcomes more than acute-phase activity. From that perspective, the LORA ocular phenotype, with its lower autoantibody load and higher environmental exposure, is best managed with tobacco-cessation counseling and proactive lid-margin care, whereas EORA requires tighter coordination with rheumatology regarding biologic therapy and screening for secondary Sjögren overlap (16).

Our 40% ANA positivity rate in EORA, although not statistically significant, is clinically noteworthy. Combined with the higher frequency of positive Schirmer tests in EORA (9.5%) and the more pronounced subjective symptoms in EORA, this pattern suggests an under-recognized overlap with secondary Sjögren disease. Sullivan et al. (16) demonstrated that meibomian gland dysfunction is a near-universal finding in primary and secondary Sjögren syndrome. In our setting, the addition of meibography to standard ocular surface evaluation is therefore likely to identify patients who would benefit from referral for Sjögren work-up, even in the absence of overt sicca complaints. Our findings add to existing evidence on dry eye severity in autoimmune rheumatic disease (25,26) and on the role of sustained inflammation in lacrimal gland injury (27). Two recent practical reviews on LORA management offer additional context for tailoring DMARD therapy in this older subgroup, where ocular adverse effects and comorbidity load demand careful coordination with rheumatology (28,29).

Study Limitations

Several limitations should be acknowledged. The study design precludes causal inference and cannot capture the progression of meibomian gland atrophy over time; recruitment from a single center limits external validity, although demographic comparability between EORA and LORA mitigates concerns about internal validity. The marked smoking imbalance between RA subgroups, combined with a moderate sample size, prevented a fully powered multivariable adjustment; the pre-specified stratified and secondary regression analyses are therefore reported as supportive rather than confirmatory, and residual confounding by methotrexate or biologic therapy cannot be excluded, although DMARD distribution did not differ between RA subgroups (18). On the instrumentation side, the Sirius+ automatic gland-atrophy segmentation has been validated in healthy subjects but not specifically in autoimmune cohorts; recent deep-learning meibography studies do, however, suggest close agreement between automatic and manual grading (11-13). Tear cytokine profiling and corneal confocal microscopy were not available, and their inclusion would have strengthened the mechanistic discussion. Given these limitations, the study is, as far as we are aware, the first direct comparison of ocular surface and meibomian gland imaging between age-matched EORA, LORA, and control groups; the rheumatologic and ophthalmologic workups were standardized, the analysis was driven by an a priori powered design with pre-specified sensitivity analyses, and meibography acquisition followed validated protocols (30).

Conclusion

Our findings suggest that EORA and LORA may represent two distinct ocular surface phenotypes. EORA was characterized by symptomatic presentation and seropositivity, with a trend toward greater meibomian gland atrophy, whereas LORA was associated with tear film instability and comparatively few symptoms. Ocular surface screening in older patients with RA should, therefore, be guided by objective meibography rather than symptom scoring alone.

Ethics

Ethics Committee Approval: This study was approved by the Usak University Non-Interventional Studies Ethics Committee (approval number: 907-907-12, date: 23.10.2025).

Informed Consent: Written informed consent was waived because of the retrospective design.

Footnotes

Authorship Contributions

Surgical and Medical Practices: I.M.U.B., A.B., Concept: I.M.U.B., A.B., Design: I.M.U.B., A.B., Data Collection or Processing: I.M.U.B., A.B., Analysis or Interpretation: I.M.U.B., A.B., Literature Search: A.B., Writing: I.M.U.B., A.B.

Conflict of Interest: The authors declared that there were no conflicts of interest.

Financial Disclosure: The authors declared that this study received no financial support.

References

1. Lee DM, Weinblatt ME. Rheumatoid arthritis. Lancet. 2001;358:903-11.
2. Uke P, Maharaj A, Adebajo A. A review on the epidemiology of rheumatoid arthritis: an update and trends from current literature. Best Pract Res Clin Rheumatol. 2025;39:102036.
3. Ma S, Wu X, Zhang X, Li K. Elderly-onset rheumatoid arthritis as a distinct entity: mechanisms, manifestations, and treatment. Curr Opin Immunol. 2026;99:102721.
4. Lehoczki A, Ungvari Z, Szappanos Á, Fekete M, Gunkl-Tóth L, Nagy G. Geroscience insights into difficult-to-treat rheumatoid arthritis: the role of unhealthy aging, comorbidity, and therapeutic complexity. Geroscience. 2026;48:2153-77.
5. Yang M, Xu F, Zhang B, Pi H. Age-stratified treatment response in rheumatoid arthritis: a systematic review, meta-analysis, and integrated genetic and single-cell evidence implicating IL6R/TYK2 signaling. Clin Rheumatol. 2026;45:2583-600.
6. Aziz NN, Hassan RM, Ibrahim RA, Afifi N, Thabet RN. Clinical and sonographic pattern of late-onset and early-onset rheumatoid arthritis: comparative study. Clin Med Insights Arthritis Musculoskelet Disord. 2026;19:11795441261429109.
7. Zimba O, Baimukhamedov C, Kocyigit BF. Late-onset rheumatoid arthritis: clinical features, diagnostic challenges, and treatment approaches. Rheumatol Int. 2025;45:152.
8. Ruiz-Lozano RE, Prida-Espaillat LA, Moll-Auais RA, et al. Ocular inflammatory manifestations in patients with rheumatoid arthritis. Reumatol Clin (Engl Ed). 2025;21:501891.
9. Turk MA, Hayworth JL, Nevskaya T, Pope JE. Ocular manifestations in rheumatoid arthritis, connective tissue disease, and vasculitis: a systematic review and metaanalysis. J Rheumatol. 2021;48:25-34.
10. Sparks JA, Karlson EW. The roles of cigarette smoking and the lung in the transitions between phases of preclinical rheumatoid arthritis. Curr Rheumatol Rep. 2016;18:15.
11. Wang J, Graham AD, Yu SX, Lin MC. Predicting demographics from meibography using deep learning. Sci Rep. 2022;12:15701.
12. Yesilirmak N, Okbay V, Yesilirmak Y, et al. Evaluation of meibomian gland dysfunction with deep learning model considering different datasets and gland morphology. Comput Biol Med. 2025;195:110679.
13. Swiderska K, Blackie CA, Maldonado-Codina C, Morgan PB, Read ML, Fergie M. A deep learning approach for meibomian gland appearance evaluation. Ophthalmol Sci. 2023;3:100334.
14. Vignesh AP, Srinivasan R. Ocular manifestations of rheumatoid arthritis and their correlation with anti-cyclic citrullinated peptide antibodies. Clin Ophthalmol. 2015;9:393-7.
15. Korkmaz C, Us T, Kaşifoğlu T, Akgün Y. Anti-cyclic citrullinated peptide (CCP) antibodies in patients with long-standing rheumatoid arthritis and their relationship with extra-articular manifestations. Clin Biochem. 2006;39:961-5.
16. Sullivan DA, Dana R, Sullivan RM, et al. Meibomian gland dysfunction in primary and secondary Sjögren syndrome. Ophthalmic Res. 2018;59:193-205.
17. Khandelwal P, Liu S, Sullivan DA. Androgen regulation of gene expression in human meibomian gland and conjunctival epithelial cells. Mol Vis. 2012;18:1055-67.
18. Sevimli N, Karadag R, Madenci E, et al. Ocular surface findings in patients with rheumatoid arthritis under methotrexate or biological agent therapy. Cutan Ocul Toxicol. 2017;36:48-51.
19. Targońska-Stępniak B, Grzechnik K, Kolarz K, Gągoł D, Majdan M. Systemic inflammatory parameters in patients with elderly-onset rheumatoid arthritis (EORA) and young-onset rheumatoid arthritis (YORA)-an observational study. J Clin Med. 2021;10:1204.
20. Ağın A, Kocabeyoğlu S, Çolak D, İrkeç M. Ocular surface, meibomian gland alterations, and in vivo confocal microscopy characteristics of corneas in chronic cigarette smokers. Graefes Arch Clin Exp Ophthalmol. 2020;258:835-41.
21. van Wesemael TJ, Morton FR, Heutz JW, et al. Smoking as a risk factor for rheumatoid arthritis: predominant association with IgA autoantibodies - comprehensive analysis of anti-modified protein antibodies with smoking and genetic risk factors in rheumatoid arthritis. Arthritis Res Ther. 2025;27:101.
22. Schargus M, Wolf F, Tony HP, Meyer-Ter-Vehn T, Geerling G. Correlation between tear film osmolarity, dry eye disease, and rheumatoid arthritis. Cornea. 2014;33:1257-61.
23. Ma W, Wang G, Li X, et al. Study of factors influencing dry eye in rheumatoid arthritis. J Ophthalmol. 2020;2020:5768679.
24. Bitirgen G, Kucuk A, Ergun MC, Satirtav G, Malik RA. Corneal nerve loss and increased Langerhans cells are associated with disease severity in patients with rheumatoid arthritis. Eye (Lond). 2023;37:2950-5.
25. Liu Y, Wu M, Ren Y, et al. Evaluation of dry eye severity and ocular surface inflammation in patients with autoimmune rheumatic diseases. Ocul Immunol Inflamm. 2024;32:2018-30.
26. Yu K, Bunya V, Maguire M, Asbell P, Ying GS; Dry Eye Assessment and Management Study Research Group. Systemic conditions associated with severity of dry eye signs and symptoms in the dry eye assessment and management study. Ophthalmology. 2021;128:1384-92.
27. Villani E, Galimberti D, Del Papa N, Nucci P, Ratiglia R. Inflammation in dry eye associated with rheumatoid arthritis: cytokine and in vivo confocal microscopy study. Innate Immun. 2013;19:420-7.
28. Yoshimi R, Nakajima H. The characteristics and management considerations of late-onset rheumatoid arthritis. Intern Med. 2024;63:3267-9.
29. Kojima M, Sugihara T, Kawahito Y, et al. Consensus statement on the management of late-onset rheumatoid arthritis. Mod Rheumatol. 2024;34:1095-102.
30. Finis D, Ackermann P, Pischel N, et al. Evaluation of meibomian gland dysfunction and local distribution of meibomian gland atrophy by non-contact infrared meibography. Curr Eye Res. 2015;40:982-9.